

# Single-Switch Buck Converter with a Ripple-Free Inductor Current

Hyun-Lark Do<sup>†</sup>

<sup>†</sup> Dept. of Electronic and Information Eng., Seoul National University of Science and Technology, Seoul, Korea

## Abstract

This paper presents a single-switch buck converter with a ripple-free inductor current. In the proposed converter, the filter inductor current ripple is completely removed by utilizing an auxiliary circuit consisting of an additional winding of the filter inductor, an auxiliary inductor, and an auxiliary capacitor. Moreover, the ripple-free current characteristic is maintained under both light load and full load conditions. The theoretical analysis and performance of the proposed converter were verified with a 110W experimental prototype operating at a 107 kHz switching frequency.

**Key Words:** Buck converter, Coupled inductor, Current ripple, DC-DC converter

## I. INTRODUCTION

Non-isolated DC-DC converters such as buck, boost, and buck-boost converters are widely used in various industrial applications. If there is a requirement for a step-down function, a buck converter is the simplest solution [1]–[5]. In a buck converter, a LC low pass filter on the output stage provides a smoothing action so that the output voltage has a limited ripple. However, a very low ripple in the current and the output voltage requires a large LC filter. Recently, the multiphase interleaving technique has been intensively studied to reduce switching ripples in the current and output voltage [2]–[8]. However, multiphase interleaved structures require many components to obtain a low ripple characteristic. Moreover, the interleaving operation of multiple converters requires complicated control techniques. In order to obtain a current balance, the use of expensive digital controllers can not be avoided. In [9], a multi-level conversion topology is suggested. However, it has similar drawbacks.

In order to overcome these problems, a single-switch buck converter with a ripple-free inductor current is suggested. By utilizing an auxiliary circuit consisting of a LC and an additional winding of the filter inductor, the ripple component of the filter inductor is dramatically reduced. In Fig. 1, the proposed buck converter is shown. The shaded area is the auxiliary circuit for achieving the current ripple cancellation. The proposed buck converter shows the ripple-free characteristic under light and full load conditions. A theoretical analysis is provided and it is verified by an 110W experimental prototype

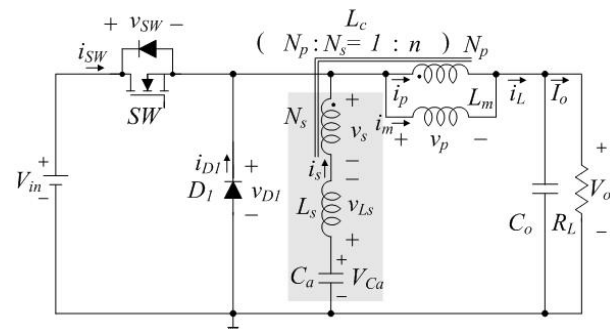


Fig. 1. Proposed buck converter.

with 100V-to-48V conversion.

This paper is organized as follows. An analysis of the proposed converter is provided in Section II. The experimental results are shown in Section III and some conclusions are given in Section IV.

## II. ANALYSIS OF THE PROPOSED CONVERTER

Fig. 1 shows a circuit diagram of the proposed buck converter. The auxiliary circuit in the shaded area includes an additional winding  $N_s$  of the filter inductor  $L_c$ , a serial inductor  $L_s$ , and an auxiliary capacitor  $C_a$ . The coupled inductor  $L_c$  is modelled as a magnetizing inductance  $L_m$  and an ideal transformer which has a turn ratio of  $N_p : N_s (= 1 : n)$ . The leakage inductance of the coupled inductor  $L_c$  is included in the serial inductor  $L_s$ . The auxiliary capacitor  $C_a$  acts as a dc-blocking capacitor. The capacitance of  $C_a$  is large enough, that  $C_a$  can be considered as a voltage source  $V_{Ca}$  during a switching period. Since the average of the voltage across the inductor should be zero at the steady state according to the volt-second balance law, the average value of the auxiliary capacitor voltage is equal to the output voltage  $V_o$ . In Fig. 2 and 3, the theoretical waveforms of the proposed buck

Manuscript received Nov. 13, 2010; revised May 4, 2011

Recommended for publication by Associate Editor Byung-Cho Choi.

<sup>†</sup> Corresponding Author: hldo@snut.ac.kr

Tel: +82-2-970-6463, Fax: +82-2-979-7903, Seoul Nat'l Univ. of Science and Tech.

Dept. of Electronic & Information Eng., Seoul National Univ. of Science and Technology, Korea

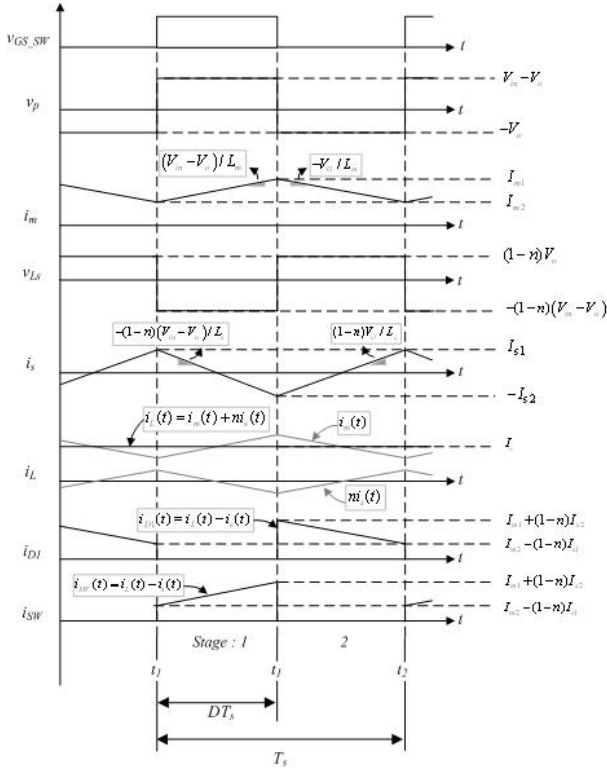


Fig. 2. Theoretical waveforms in mode A.

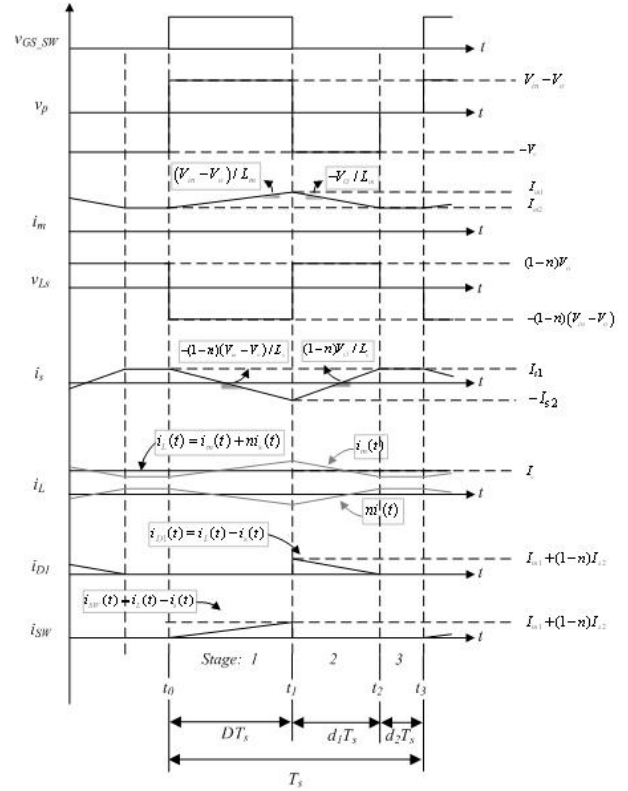


Fig. 3. Theoretical waveforms in mode B.

converter are shown. Mode A corresponds to the continuous conduction mode of a conventional buck converter. Mode B corresponds to the discontinuous conduction mode. Fig. 4 shows the operating stages. Mode A consists of stage 1 and 2 during a switching period  $T_s$ . Mode B consists of stage 1 through 3 during  $T_s$ .

#### A. Mode A

Stage 1  $[t_0, t_1]$ : This stage starts at  $t_0$  with the turn-on of the switch SW. Since the voltage  $v_p$  across  $L_m$  is  $V_{in} - V_o$ , the magnetizing current  $i_m$  increases from its minimum value  $I_{m2}$  linearly with a slope of  $(V_{in} - V_o)/L_m$  as follows:

$$i_m(t) = I_{m2} + \frac{V_{in} - V_o}{L_m} (t - t_0). \quad (1)$$

In this stage, the voltage  $v_{Ls}$  across  $L_s$  is  $-(1-n)(V_{in} - V_o)$ . As a result, the current  $i_s$  decreases linearly from its maximum value  $I_{s1}$  with a slope of  $-(1-n)(V_{in} - V_o)/L_s$  as follows:

$$i_s(t) = I_{s1} - \frac{(1-n)(V_{in} - V_o)}{L_s} (t - t_0). \quad (2)$$

Since  $i_L = i_m + i_p = i_m + ni_s$  from Fig. 1, the filter inductor current  $i_L$  can be written as follows:

$$i_L(t) = I_{m2} + nI_{s1} + \left( \frac{V_{in} - V_o}{L_m} - \frac{(1-n)(V_{in} - V_o)}{L_s} \right) (t - t_0). \quad (3)$$

From (3), the inductor current ripple can be cancelled out and  $i_L$  can be constant as  $I_{m2} + nI_{s1}$  by satisfying the following condition:

$$L_s = n(1-n)L_m. \quad (4)$$

Stage 2  $[t_1, t_2]$ : At  $t_1$ , SW is turned off and stage 2 starts. Since  $v_p$  is  $-V_o$ ,  $i_m$  decreases from its maximum value  $I_{m1}$  with a slope of  $-V_o/L_m$  as follows:

$$i_m(t) = I_{m1} - \frac{V_o}{L_m} (t - t_1). \quad (5)$$

The voltage  $v_{Ls}$  is  $(1-n)V_o$  in this stage. Therefore,  $i_{Ls}$  increases from its minimum value  $-I_{s2}$  with a slope of  $(1-n)V_o/L_s$  as follows:

$$i_s(t) = -I_{s2} + \frac{(1-n)V_o}{L_s} (t - t_1). \quad (6)$$

From (5) and (6), the filter inductor current  $i_L$  can be rewritten as follows:

$$i_L(t) = I_{m1} - nI_{s2} + \left( -\frac{V_o}{L_m} + \frac{n(1-n)V_o}{L_s} \right) (t - t_1). \quad (7)$$

Due to condition (4), the ripple component in (7) is cancelled out and the current  $i_L$  is constant as  $I_{m1} - nI_{s2}$ . From (4), (6), and (7), the diode current  $i_{D1}$  is obtained as follows:

$$i_{D1}(t) = I_{m1} + (1-n)I_{s2} - \frac{(1-n)V_o}{L_s} (t - t_1). \quad (8)$$

Referring to the voltage waveforms  $v_p$  across the magnetizing inductance  $L_m$ , shown in Fig. 2, the volt-second balance law gives:

$$(V_{in} - V_o)DT_s - V_o(1-D)T_s = 0. \quad (9)$$

Equation (9) can be rewritten as follows:

$$\frac{V_o}{V_{in}} = D. \quad (10)$$

Since the average value of the current flowing through a capacitor should be zero at the steady-state,  $I_{s1}$  is equal to  $I_{s2}$ . As a result,  $I_{s1}$  and  $I_{s2}$  can be obtained from (6) as follows:

$$I_{s1} = I_{s2} = \frac{(1-n)(1-D)V_o T_s}{2L_s}. \quad (11)$$

Since the average value of  $i_s$  is zero, the average value of  $i_L$  is equal to the average value of  $i_m$ , which is  $(I_{m1} + I_{m2})/2$ . Also, the average current flowing through the output capacitor  $C_o$  is zero. Therefore,  $I_{m1}$  and  $I_{m2}$  can be easily calculated by:

$$I_{m1} = I_o + \frac{(V_{in} - V_o)DT_s}{2L_m}, \quad (12)$$

$$I_{m2} = I_o - \frac{(V_{in} - V_o)DT_s}{2L_m}. \quad (13)$$

Therefore, it can be easily seen that  $I_{m2} + nI_{s1}$  is equal to  $I_{m1} - nI_{s2}$  from (11), (12), and (13). The ripple component of the inductor current  $i_L$  is completely removed in mode A by satisfying condition (4).

### B. Mode B

Stage 1  $[t_0, t_1]$ : This stage is identical to stage 1 of mode A. The magnetizing current  $i_m$  increases from its minimum value  $I_{m2}$  linearly with the same slope and the current  $i_s$  decreases linearly from its maximum value  $I_{s1}$  with the same slope as in stage 1 of mode A. The inductor current ripple can be cancelled out and  $i_L$  can be constant as  $I_{m2} + nI_{s1}$  by satisfying condition (4).

Stage 2  $[t_1, t_2]$ : This stage is identical to stage 2 of mode A. All of the currents and voltages equations are equal to those in stage 2 of mode A.

Stage 3  $[t_2, t_3]$ : At  $t_2$ , the diode current  $i_{D1}$  arrives at zero and the diode  $D_1$  is turned off. From Fig. 4, the following relations can be obtained by:

$$v_{Ls} + (1-n)v_p = 0, \quad (14)$$

$$(1-n)i_s = i_m. \quad (15)$$

Equations (14) and (15) can be rewritten as follows:

$$L_s \frac{di_s}{dt} + (1-n)L_m \frac{di_m}{dt} = 0, \quad (16)$$

$$(1-n) \frac{di_s}{dt} = \frac{di_m}{dt}. \quad (17)$$

From (16) and (17), the following relation can be obtained by:

$$(L_s + (1-n)^2 L_m) \frac{di_s}{dt} = 0. \quad (18)$$

From (18), it can be seen that  $di_s/dt = 0$ . Therefore, in this stage, the voltages  $v_{Ls}$  and  $v_p$  are zero and the currents  $i_s$  and  $i_m$  are maintained as  $I_{s1}$  and  $I_{m2}$ , respectively. The filter inductor current  $i_L$  is determined by:

$$i_L = I_{s1} = nI_{s1} + I_{m2}. \quad (19)$$

Referring to the voltage waveforms  $v_p$  across the magnetizing inductance  $L_m$ , shown in Fig. 3, the volt-second balance law gives:

$$(V_{in} - V_o)DT_s - V_o d_1 T_s = 0. \quad (20)$$

Equation (20) can be rewritten as follows:

$$\frac{V_o}{V_{in}} = \frac{D}{D + d_1}. \quad (21)$$

Since the current  $i_s$  increases from  $-I_{s2}$  to  $I_{s1}$  during stage 2, the following relation is obtained by:

$$I_{s1} = -I_{s2} + \frac{(1-n)V_o d_1 T_s}{L_s}. \quad (22)$$

The diode current  $i_{D1}$  decreases from  $I_{m1} + (1-n)I_{s2}$  to zero. It determines the following relation:

$$0 = I_{m1} + (1-n)I_{s2} - \frac{(1-n)V_o}{L_s} d_1 T_s. \quad (23)$$

From (19), (22), and (23), the following relation can be obtained by:

$$I_{m1} - nI_{s2} = I_{m2} + nI_{s1}. \quad (24)$$

From (24), the ripple component of the inductor current  $i_L$  is completely removed in mode B under condition (4). Since the ripple component of the current  $i_L$  is removed, the current  $i_L$  is always equal to the output current  $I_o$ . The minimum and maximum values  $I_{s1}$ ,  $I_{s2}$ ,  $I_{m1}$ , and  $I_{m2}$  are calculated by:

$$I_{s1} = I_o, \quad (25)$$

$$I_{s2} = -I_o + \frac{(1-n)V_o d_1 T_s}{L_s}, \quad (26)$$

$$I_{m1} = (1-n)I_o + \frac{n(1-n)V_o d_1 T_s}{L_s}, \quad (27)$$

$$I_{m2} = (1-n)I_o. \quad (28)$$

### C. Mode A Operation Condition

The boundary for mode A operation is found by setting the minimum value of the diode current  $i_{D1}$  to zero. This defines a minimum value of  $L_s$  or  $L_m$ . Using (8), the following relation is obtained by:

$$0 = I_{m1} + (1-n)I_{s2} - \frac{(1-n)V_o}{L_s^*} (1-D)T_s, \quad (29)$$

where  $L_s^*$  is the minimum value of  $L_s$  for mode A operation. Solving (29) with (11) gives:

$$L_s^* = \frac{(1-n)V_o}{I_o} (1-D)T_s. \quad (30)$$

With (4), the minimum magnetizing inductance  $L_m^*$  for mode A operation is also obtained by:

$$L_m^* = \frac{V_o(1-D)T_s}{nI_o}. \quad (31)$$

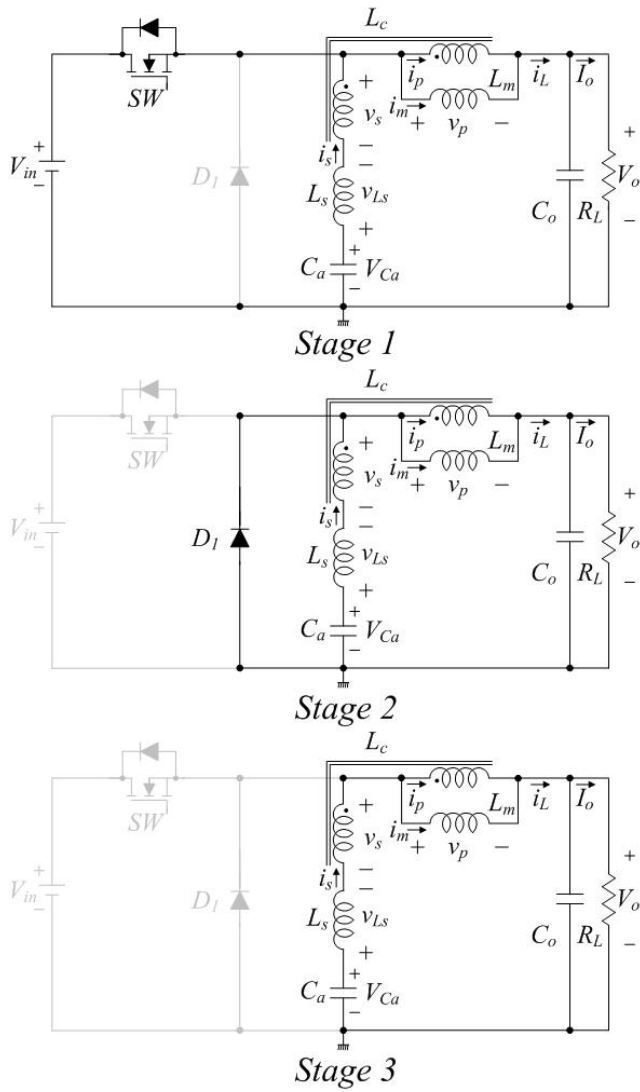
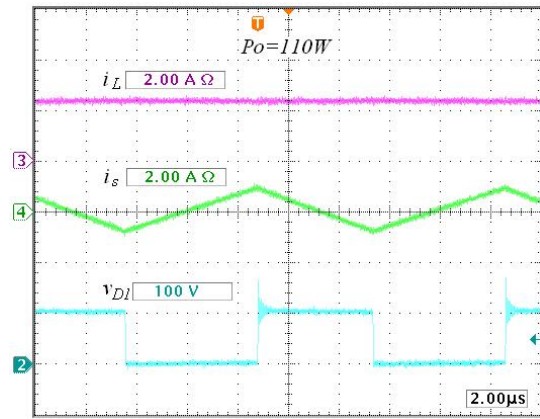


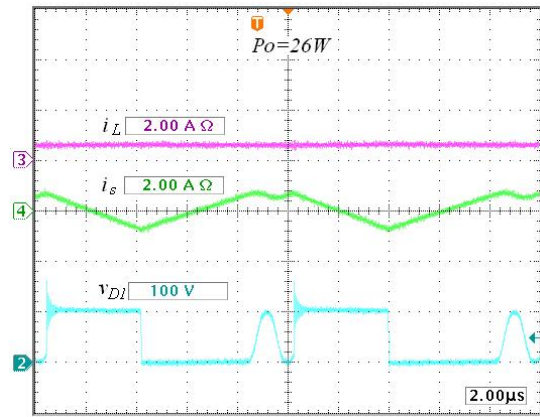
Fig. 4. Operating stages.

III. EXPERIMENTAL RESULTS

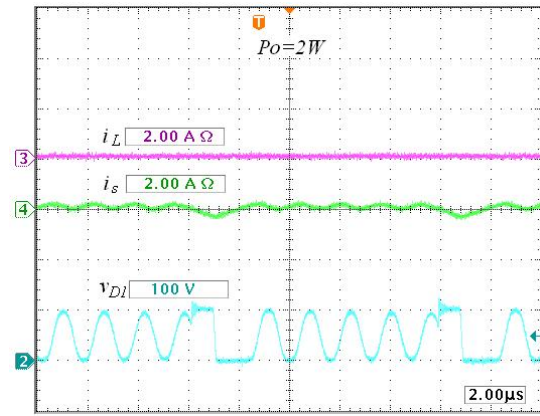
A prototype buck converter is implemented with the specifications of  $n = 0.7$ ,  $L_m = 200\mu\text{H}$ ,  $L_s = 42\mu\text{H}$ ,  $f_s = 107\text{kHz}$ ,  $V_{in} = 100\text{V}$ ,  $V_o = 48\text{V}$ , and  $P_o = 110\text{W}$ . Fig. 5 shows the experimental waveforms. These waveforms show that the ripple components of the filter inductor current  $i_L$  are completely cancelled out regardless of the load condition. Under a light load, the proposed converter operates in mode B. Like a conventional buck converter, a parasitic resonance occurs in mode B operation, but it does not affect the inductor current ripple. Fig. 6 shows the output ripple voltages of the proposed converter. The measured efficiency of the proposed buck converter is plotted in Fig. 7 and compared with a conventional buck converter. The conventional buck converter is implemented with the same circuit parameters except for the auxiliary circuit. In the proposed converter, the auxiliary circuit may cause additional conduction losses. However, the ripple-free inductor current can reduce the power lost due to the equivalent series resistance of the output capacitor. Eventually, the efficiency curves are quite similar. If a conventional buck converter is designed to meet the same ripple current criterion,



(a)



(b)



(c)

Fig. 5. Experimental waveforms. (a)  $P_o = 110\text{W}$ , (b)  $P_o = 26\text{W}$ , (c)  $P_o = 2\text{W}$ .

its efficiency may be worse than that of the proposed converter due to its large LC filter.

IV. CONCLUSIONS

A single-switch buck converter with a ripple-free inductor current was proposed. The auxiliary circuit can cancel out the ripple component of the inductor current completely. Regardless of the load condition, its ripple-free characteristic is maintained. The overall efficiency is similar to that of a conventional converter. A low current and voltage ripple is accomplished without sacrificing simplicity.

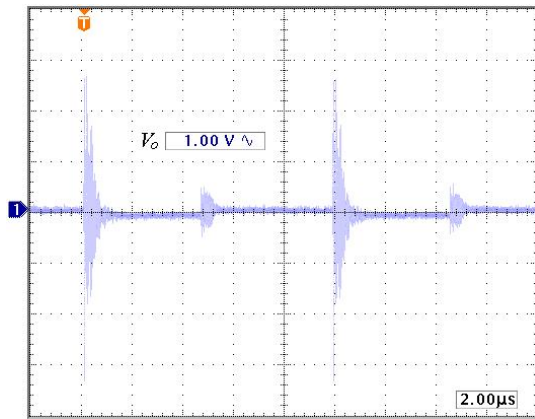


Fig. 6. Output ripple voltage of the proposed converter.

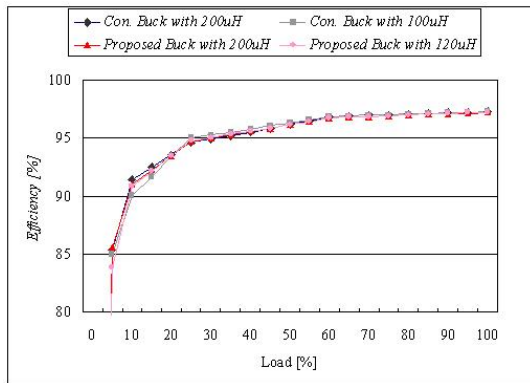


Fig. 7. Measured efficiency.

## REFERENCES

[1] E. Rokhsat-Yazdi, A. Afzali-Kusha, and M. Pedram, "A high-efficiency, auto mode-hop, variable-voltage, ripple control buck converter," *Journal*

*of Power Electronics*, Vol. 10, No. 2, pp. 115-124, Mar. 2010.

- [2] P. Xu, J. Wei, and F. C. Lee, "Multiphase coupled-buck converter-a novel high efficient 12V voltage regulator module," *IEEE Trans. Power Electron.*, Vol. 18, No. 1, pp. 74-82, Jan. 2003.
- [3] B. R. Lin and C. L. Huang, "Interleaved ZVS converter with ripple-current cancellation," *IEEE Trans. Ind. Electron.*, Vol. 55, No. 4, pp. 1576-1585, Apr. 2008.
- [4] J.-H. Kim, J.-G. Lim, S.-K. Chung, and Y.-J. Song, "DSP-based digital controller for multi-phase synchronous buck converters," *Journal of Power Electronics*, Vol. 9, No. 3, pp. 410-416, May 2009.
- [5] M. Veerachary, "Performance improvement of voltage-mode controlled interleaved buck converters," *Journal of Power Electronics*, Vol. 5, No. 2, pp. 104-108, Apr. 2005.
- [6] S. Abedinpour, B. Bakaloglu, and S. Kiaei, "A multistage interleaved synchronous buck converter with integrated output filter in 0.18  $\mu\text{m}$  SiGe process," *IEEE Trans. Power Electron.*, Vol. 22, No. 6, pp. 2164-2175, Nov. 2007.
- [7] J. Choi, H. Cha, and B.-M. Han, "A three-phase interleaved DC-DC converter with active clamp for fuel cells," *IEEE Trans. Power Electron.*, Vol. 25, No. 8, pp. 2115-2123, Aug. 2010.
- [8] W. Li and X. He, "A family of interleaved boost and buck converters with winding-cross-coupled inductors," *IEEE Trans. Power Electron.*, Vol. 23, No. 6, pp. 3164-3173, Nov. 2008.
- [9] Y. Tao and S.-J. Park, "A novel ripple-reduced DC-DC converter," *Journal of Power Electronics*, Vol. 9, No. 3, pp. 396-402, May 2009.



**Hyun-Lark Do** received his B.S. from Hanyang University, Seoul, Korea, in 1999, and his M.S. and Ph.D. in Electronic and Electrical Engineering from the Pohang University of Science and Technology, Pohang, Korea, in 2002 and 2005, respectively. From 2005 to 2008, he was a Senior Research Engineer with the PDP Research Laboratory, LG Electronics Inc., Gumi, Korea. Since 2008, he has been with the Department of Electronic and Information Engineering, Seoul National University of Science and Technology, where he is currently a Professor. His research interests include the modeling, design, and control of power converters, soft-switching power converters, resonant converters, power factor correction circuits, and driving circuits for plasma display panels.